

# Electrooxidation of stainless steel AISI 304 in carbonate aqueous solution at pH 8

M. DROGOWSKA, H. MÉNARD

*Département de Chimie, Université de Sherbrooke, Sherbrooke, Québec, Canada J1K 2R1*

L. BROSSARD

*Institut de Recherche d'Hydro-Québec (IREQ), Varennes, Québec, Canada J3X 1S1*

Received 6 September 1994; revised 26 June 1995

The electrochemical behaviour of stainless steel AISI 304 (SS304) has been investigated in deaerated 0.1–1 M NaHCO<sub>3</sub> solutions at pH 8 using a rotating disc electrode. The polarization curves are characterized by a broad range of passivity at low potentials (–0.8 to 0.3 V), a depassivation region at 0.4 V vs SCE and, at high potentials (0.5 to 0.85 V), a passive region before oxygen evolution. In the low potential range, the SS304 electrode behaves like a Cr-rich metallic phase, and the dissolution of Fe<sup>2+</sup> ions into the solution is hindered by the formation of a Cr<sub>2</sub>O<sub>3</sub> layer. As the potential reaches 0.4 V, the oxidation–dissolution of Cr(III) oxide/hydroxide to CrO<sub>4</sub><sup>2–</sup> ions occurs, with the participation of bicarbonate/carbonate as a catalyst in the dissolution reaction. Since the chromium oxide/hydroxide dissolution and subsequent surface enrichment of iron oxides occur, the applied potential, exposure time and oxidation charge have a considerable effect on the passive film properties. At high potentials, the presence of a passive film of iron oxides/hydroxides or oxyhydroxides plays a key role in the SS304 passivity with the presence of Fe(VI) species incorporated or adsorbed into the passive films. Colouration of the SS304 surface is observed in the second passive region. A film of a uniform gold colour formed on SS304, mild steel 1024 and iron in carbonate and borate solutions at pH 8. The colour of the electrode surfaces remain unchanged in air and in solutions at positive potential but it disappears at open-circuit potential or is easily reduced in the first negative-going potential scan.

## 1. Introduction

The corrosion of iron is a multistep process and it is almost impossible to establish the true steady state of passive iron in neutral solutions [1–4]. The composition of passive films depends on the potential of the iron, the pH of the solution and the identity of the anions present. First, in slightly alkaline solutions layers of Fe(OH)<sub>2</sub> formed, which, after passivation, are oxidized to mixed valence iron oxides, hydroxides and oxyhydroxides. A small amount of anions may be incorporated into the passive layer. Considering the complete miscibility of these oxides, it would not be justified to assume a boundary phase between Fe<sub>3</sub>O<sub>4</sub> and γ-Fe<sub>2</sub>O<sub>3</sub>, although there are significant differences between the inner and outer layers. The stoichiometry and distribution of cationic and anionic species in the crystallographic lattice of an oxide are still controversial subjects, even in the widely studied borate buffer solution. It has been suggested that the constituents of passive films are either microcrystalline or amorphous.

The characterization of passive films on stainless steel remains far from clarified. The thermodynamic data are complex and the structural organization is still difficult. The electronic structure of passive layers on stainless steel has not been established. Some

studies have been published on the electrochemical behaviour of stainless steel in acidic solutions [5–12] and in neutral aqueous media [12–18]. Photochemical and photoelectrochemical techniques [18–21] have been used to obtain *in situ* information about the electronic properties of passive films. The different behaviour exhibited by various stainless steels is attributed to the different structure and highly defective nature of passive films.

Recently, application of surface analytical techniques such as XPS, Auger, SIMS and XANES have provided information on the atomic composition of passive films formed on steel. For example, they have revealed that passive oxide films on iron–chromium alloys consist predominantly of chromium oxide/oxyhydroxide with a thickness ~ 1–3 nm and at higher anodic potentials in transpassive region some Cr<sup>6+</sup> ions can be incorporated. The presence of cations of iron and other alloying elements and incorporated anions in the films is also generally accepted, although their structure and chemical composition remain unknown. The Ni<sup>2+</sup> content in a passive film is low, and the metallic state of nickel dominates [23]. A small loss of nickel seems to occur with chromium dissolution in the second passive region, although this amount is significantly less than either Fe or Cr, and Ni becomes enriched at

the surface [24]. The results of surface analysis indicated very significant differences between the *ex situ* and *in situ* films, suggesting that high vacuum condition for *ex situ* examination does lead to major structural changes.

Nonaggressive anions in the solution play an important role in the passivation process. Although carbon dioxide is commonly present in all water systems and in the oil and gas industry, the corrosion resistance of stainless steel in carbonate solutions has seldom been studied. The objective of this work, therefore, was to investigate the electrochemical behaviour of passive films formed on stainless steel AISI 304 (SS304) in deaerated carbonate/bicarbonate solutions at pH 8. The voltammetric characteristics of surface films formed on SS304 and chromium were studied with the aid of a rotating disc electrode, paying a special attention to the composition and properties of passive films formed on SS304 at potentials above 0.4 V.

## 2. Experimental details

The study was made using austenitic stainless steel AISI 304 (SS304) with the following chemical composition (wt %): C 0.009, Mn 1.67, P 0.034, S 0.020, Si 0.51, Cu 0.35, Ni 8.2, Cr 19.4, V 0.07, Mo 0.30, Co 0.14, Sn 0.018, Al 0.006, Ti 0.006, Nb 0.033 and balance Fe. To compare the results, some measurements with the main components of SS304 were also performed. Specimens of iron (Johnson Matthey), nickel (Johnson Matthey) and chromium (99.99%, Omega) were machined in the shape of a cylinder and one of the tops of the cylinder was set in a Kelf holder which constituted the working rotating disc electrode. The exposed surface area was 0.13 cm<sup>2</sup>. The electrodes were mechanically polished with an alumina suspension to a mirror-like finish and rinsed with distilled water. The electrode surface was examined before and after the experiments using a Bausch & Lomb optical microscope (70×). At the beginning of each experiment, the electrode was immersed in the solution with the potentiostat set at -0.9 V and cathodically polarized to remove some of the surface oxides. A base rotation speed of 1000 r.p.m. was used. The auxiliary electrode was a platinum grid, which was separated from the main compartment by a Nafion<sup>®</sup> membrane. A saturated calomel electrode (SCE) connected to the cell by a bridge with a Luggin capillary served as the reference electrode. All potentials quoted in the paper refer to this electrode. The potential was corrected for the *iR* drop which was measured by the a.c. impedance method.

The solutions were prepared from analytical grade materials (BDH) and deionized water. The pH value was 8, by adding NaOH as necessary. A borate buffer of pH 8.4 was prepared from 7.07 g H<sub>3</sub>BO<sub>3</sub> + 8.17 g Na<sub>2</sub>B<sub>4</sub>O<sub>7</sub>·10 H<sub>2</sub>O per litre. The cell capacity was ~600 ml, which ensured that the build-up of dissolved ions in the bulk of the solution would be negligible during the course of a given experiment. All solutions

were deaerated before each experiment using high-purity nitrogen and were purged continuously during the measurements. All experiments were performed at room temperature.

The measurements were made using a Princeton Applied Research (PAR) model 273 A galvanostat-potentiostat controlled by a PC using M270 PAR electrochemical software. The electrode was rotated using a Pine Instrument or PAR electrode rotator.

## 3. Results and discussion

### 3.1. Preliminary experiments

Figures 1 and 2 show the potentiodynamic *i/E* curves and the corrosion potentials against time dependence for SS304, iron, chromium and nickel rotating-disc electrodes in 1 M NaHCO<sub>3</sub> solutions at pH 8. The electrode rotated at 1000 r.p.m. and the scan rate was 20 mV s<sup>-1</sup>. For all four metals, the passive film formed on the electrodes was not completely reduced, regardless of the cathodic potential applied. The anodic activity of the electrodes at negative potentials, which is attributed to hydrogen adsorption, increased as the reduction potential became more negative or the reduction time increased, as illustrated in Fig. 3 for the SS304 electrode in 0.1 M NaHCO<sub>3</sub> solution rotated at 1000 r.p.m. and  $dE/dt = 0.005 \text{ V s}^{-1}$ . After each experiment, the electrode surface was examined through an optical microscope and no visible change was observed. As long as the rotating electrode was used, no traces of localized corrosion were detected but when the stationary electrode was used crevice corrosion was observed.

Measurements of the potential under open circuit conditions  $E_{\text{corr}}$  (Fig. 2) give information about a corrosion system not disturbed by any external voltage or current source, so that no additional corrosion effects are induced. The diagrams show the different behaviour of the metals. In the 1 M NaHCO<sub>3</sub> deaerated solution at pH 8, the potentials of -0.84 V for iron and -0.60 V for nickel electrodes remained essentially unchanged over time. According to thermodynamic data [25-27], the first iron oxidation level corresponds mainly to the fast reaction of iron(II) hydroxide/oxide formation. The SS304 and Cr electrodes, are similar in behaviour: the potential increased continuously with the exposure time, albeit at a faster rate for chromium. For example, after 9000 s,  $E_{\text{corr}}$  was -0.55 V for Cr and -0.60 V for SS304, but no stable value was reached. The  $E_{\text{corr}}$  values depend on the pretreatment of the electrode surface but the trend is unaltered. The increase in  $E_{\text{corr}}$  for the SS304 and Cr electrodes is attributed to the slow kinetics with which the oxide films reach equilibrium; it is known that Cr<sup>3+</sup> complexes react very slowly, so that a film of Cr-hydroxide can be maintained [22, 23]. The comparatively thinner oxide layers formed on the chromium surface [29] could explain the faster rate of Cr ennoblement. The similarity of the characteristics of SS304 and Cr electrodes (different from Fe and Ni electrodes) suggests

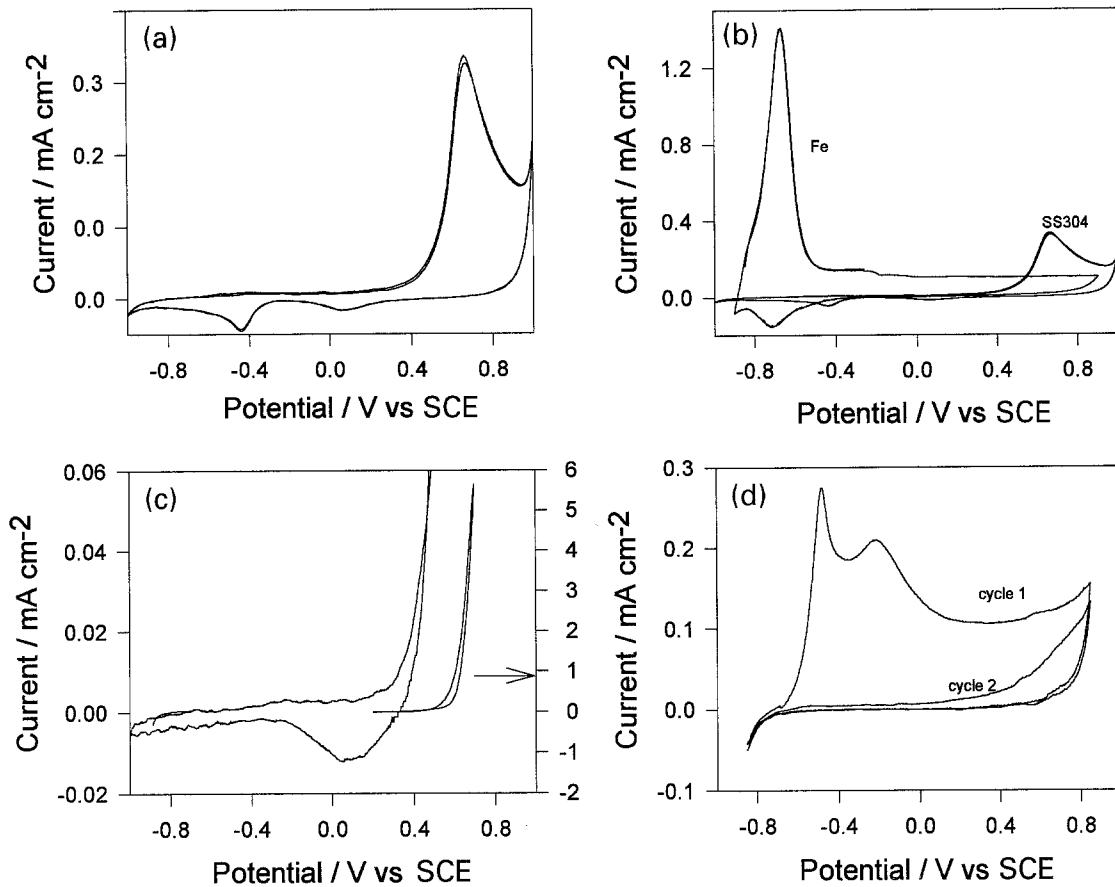


Fig. 1. Cyclic voltammograms for SS304 (a), iron (b), chromium (c) and nickel (d) electrodes, rotated at 1000 r.p.m.,  $dE/dt = 0.02 \text{ V s}^{-1}$ , in 1 M  $\text{NaHCO}_3$  solution at pH 8.

that a chromium oxide/hydroxide film forms on the SS304 surface.

### 3.2. Chromium

Thermodynamic predictions [26–28] in the form of potential-pH diagrams of a Cr- $\text{H}_2\text{O}$  system show chromium to be a very base metal, whose domain of stability is considerably lower than that of water. In the presence of neutral and slightly alkaline solutions, chromium tends to become covered with an oxide or a

hydroxide and can only dissolve as chromate ions  $\text{CrO}_4^{2-}$  at high positive potentials. A number of studies employing electrochemical and surface analytical techniques [30–36] have suggested that the passive film on chromium about 0.3–2.0 nm thick, is a trivalent oxide/hydroxide containing some water. Results from *in situ* modulation spectroscopy [29] suggest that a mixed valent Cr(III)/Cr(VI) oxide is present in the transpassive region. No evidence has been found

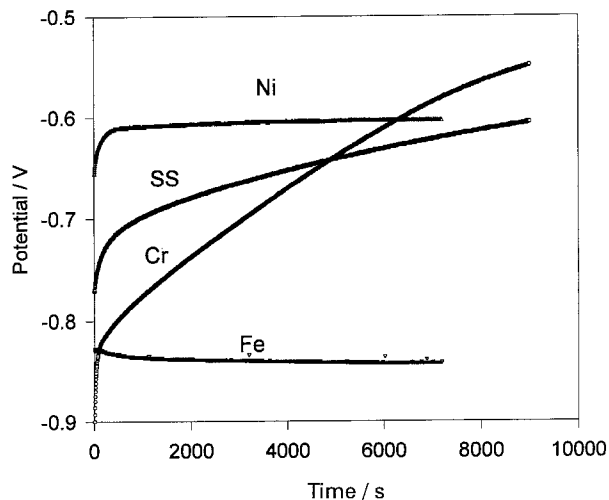


Fig. 2. Open circuit corrosion potential against time for SS304, iron, chromium and nickel electrodes, rotated at 1000 r.p.m., in 1 M  $\text{NaHCO}_3$  solution at pH 8.

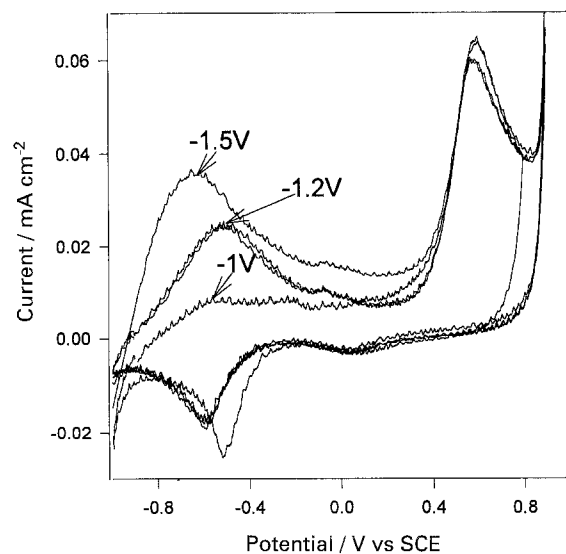


Fig. 3. Effect of negative potential scan limit on the anodic activity of the SS304 electrode rotated at 1000 r.p.m.,  $dE/dt = 0.005 \text{ V s}^{-1}$ , in 0.1 M  $\text{NaHCO}_3$  solution at pH 8. The cathodic potential scan limit was -1.5, -1.2 and -1.0 V.

for the existence of multivalent states of chromium in the passive film.

In Fig. 1(c), the chromium electrode, rotated at 1000 r.p.m. at a scan rate of  $0.02 \text{ V s}^{-1}$  in  $1 \text{ M NaHCO}_3$  solution appears to be in a passive state in the potential range from  $-1$  to  $+0.4 \text{ V}$ . At the latter potential, the anodic current increases with the applied potential without further passivation; the oxidation of  $\text{Cr(III)}$  to  $\text{Cr(VI)}$  forms a readily soluble oxide and  $\text{CrO}_4^{2-}$  ions, and the oxygen evolution may proceed simultaneously. In a subsequent negative-going potential scan the cathodic current peak appears at about  $+0.1 \text{ V}$  and slowly increased with the oxidation time at potentials greater than  $0.4 \text{ V}$ . Considering thermodynamic data [26–28] for a slightly alkaline solution at potentials greater than  $0.3 \text{ V}$ , a sufficient overpotential exists to cause dissolution of the chromium. A number of experiments were carried out with the rotating Cr electrode for various oxidation times in  $1 \text{ M NaHCO}_3$  solution and the formation of an anodic film was estimated from reduction charges. Figure 4 presents the results for electrode oxidation at  $0.45 \text{ V}$  for  $600 \text{ s}$ , and at  $0.4 \text{ V}$  for  $20 \text{ h}$  and  $72 \text{ h}$ , and subsequent cycling of the potential first in a negative then in a positive direction at a scan rate of  $0.05 \text{ V s}^{-1}$ . At the end of oxidation the solution was yellowish due to dissolved chromate. After  $20 \text{ h}$ , the anodic current  $i_a = 15 \mu\text{A cm}^{-2}$  and charges  $Q_{\text{ox}} = 700 \text{ mC cm}^{-2}$  and  $Q_{\text{red}} = 1 \text{ mC cm}^{-2}$  were measured. The surface film grew slowly during the first  $20 \text{ h}$  but from  $20 \text{ h}$  to  $72 \text{ h}$  oxidation time, the reduction wave at  $0.1 \text{ V}$  increased and a new large current maximum dominated at  $-0.45 \text{ V}$  (Fig. 4). Some electrode passivation was evidenced by a decrease in the anodic current,  $i_a$ , to  $3.3 \mu\text{A cm}^{-2}$  and an increase in the reduction charge to  $Q_{\text{red}} = 7.2 \text{ mC cm}^{-2}$  for  $Q_{\text{ox}} = 900 \text{ mC cm}^{-2}$ .

Under such circumstances, the colour of the chromium electrode surface changed to bright gold. The

layer did not adhere well (easy to remove just by rinsing with water) but once the electrode was removed from the solution and dried, the appearance of the surface remained unchanged in air. In the solution, the oxidation product was easily reduced at a cathodic current peak located at  $-0.45 \text{ V}$  and the gold colour disappeared after the first cathodic potential scan. The reduction charge was equivalent to less than 1% of the charge associated with the electrode oxidation. The reduction process of the surface film could be the transformation of  $\text{Cr}^{6+}$  to  $\text{Cr}^{3+}$ ,  $\text{Cr}^{4+}$  to  $\text{Cr}^{3+}$  or  $\text{Cr}^{6+}$  to  $\text{Cr}^{4+}$ . The shape of the reduction current peak at  $-0.45 \text{ V}$  and the nature of the surface products combined with the lack of adhesion of the products suggest that the surface film is formed by a dissolution-precipitation mechanism. A small amount of  $\text{Cr(VI)}$  species may be incorporated into the surface film and reduced at  $0.1 \text{ V}$  cathodic wave.

### 3.3. AISI 304 stainless steel

**3.3.1. Passivity at potentials below  $0.4 \text{ V}$ .** Figure 1(a) shows a region of over one volt in which the electrode is passive, then, at  $0.4 \text{ V}$ , the anodic current increases without any visible corrosion, reaches a maximum and a second passive region appears before oxygen evolution. The passivity in both potential regions was found to be independent of the carbonate concentration, indicating that passivation is due to the formation of oxides, hydroxides or oxyhydroxides films. The typical activation current maximum that appears at negative potentials during the active/passive transition on iron (Fig. 1(b)) is not present on SS304 (Fig. 1(a)) or chromium (Fig. 1(c)). At low potentials, the polarization curve of SS304 is very similar to that corresponding to Cr (Fig. 1(c)), suggesting that the passive film is composed of  $\text{Cr(III)}$  oxide/hydroxide occupying mainly the inner layer, with iron (II/III)

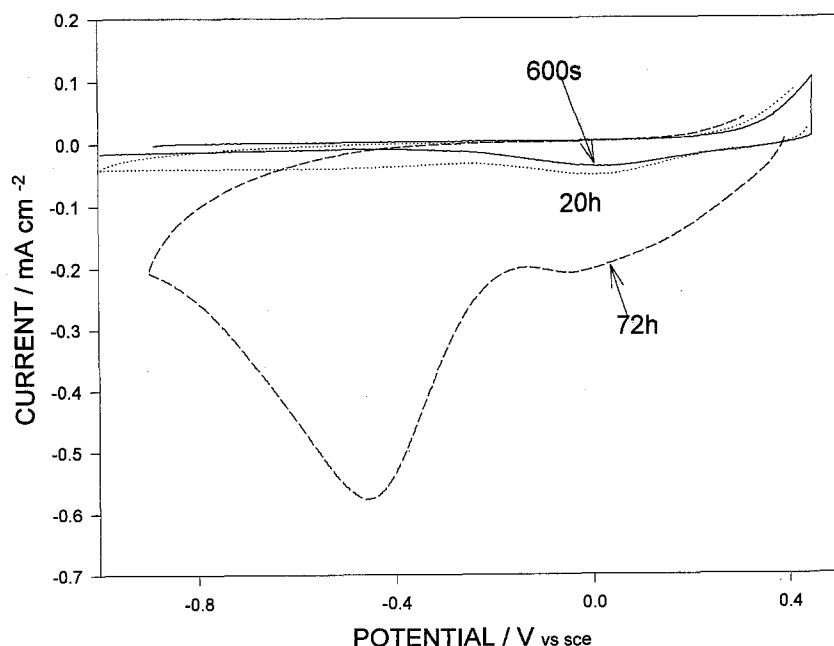


Fig. 4. Cyclic voltammograms for chromium electrode oxidized at  $0.45 \text{ V}$  for  $600 \text{ s}$ , and at  $0.4 \text{ V}$  for  $20$  and  $72 \text{ h}$ . An anodic potential step from  $-0.8 \text{ V}$  to the positive potential was applied, and the amount of oxidation product was estimated by subsequent cycling of the potential first in a negative then in a positive direction with a scan rate of  $0.05 \text{ V s}^{-1}$ . The electrode was rotated at  $1000 \text{ r.p.m.}$  in  $1 \text{ M NaHCO}_3$  solution at  $\text{pH } 8$ .

oxides, hydroxides and oxyhydroxides in the outer layers [15, 16, 44–46]. The carbonate and hydroxycarbonate mixed salt would also exist.

**3.3.2. Passivity at potentials above +0.4 V.** The voltammograms in Fig. 1(a) and 1(c) show that the electrochemical behaviour of the SS304 electrode in its second passive potential range differs from that of the Cr electrode. At the SS304 depassivation potential, 0.4 V, the anodic current increases and a maximum is observed. This current peak is found to be independent of the electrode rotation speed, which ranges from 200 to 2000 r.p.m., suggesting that the reaction rate is limited by a solid-state electrooxidation process on the surface. The rate of the anodic current increase was a linear function of the  $\text{NaHCO}_3$  concentration between 0.05 and 1 M (Fig. 5). The potential of the anodic current peak at 0.6 V remained constant, and it is deduced that the composition of the outer film is independent of the solution concentration. The voltammograms in a borate solution (Fig. 6) show similarly shaped polarization curves, however the anodic activity of SS304 electrode is found to be lower than in carbonate/bicarbonate solution at the same pH.

These considerations suggest the participation of the  $\text{HCO}_3^-/\text{CO}_3^{2-}$  ions as catalyst in the dissolution reaction, slightly affecting the passivation process. The passive film seems to contain mixed valence iron carbonate compounds, a species which may not even exist in macroscopic quantities. Structurally, the mixed valence carbonate is closely related to iron oxyhydroxide [3]. The Pourbaix diagram for Fe- $\text{CO}_2$ - $\text{H}_2\text{O}$  system [25] indicates that, in this potential region,  $\text{FeCO}_3$  would be a solid phase ( $K_{so} = 3 \times 10^{-11}$  [37]) and that passivation could occur by the transformation of  $\text{FeCO}_3$  to various Fe(III) oxides or oxyhydroxides in the passive films. The results suggest that the second passivation is due to an iron oxide/hydroxide/

oxyhydroxide film ( $\text{Fe}(\text{OH})_2$   $K_{so} = 4.9 \times 10^{-17}$ ;  $\text{Fe}(\text{OH})_3$   $K_{so} = 10^{-39}$  [37]). The chemical and electrochemical reactions are important and may be equivalent to the effect of a potential increase.

The occurrence of a critical potential at +0.4 V in the properties of passive films on stainless steels containing chromium in neutral solutions has been reported in the literature [12, 13, 21, 24, 38–43]. Photoelectrochemical studies in a  $\text{Na}_2\text{SO}_4$  solution [6, 7, 21] have revealed that passive film properties change with potential and that at +0.4 V strong changes occur not only in the magnitude of the photocurrent but also in the shape of its transient and capacitance values. Angular-dependent XPS examinations [44] of the films grown in alkaline solutions indicate an accumulation of Cr, probably composed of the Cr(III) oxide/hydroxide, in the inner part. Since  $\text{Fe}_2\text{O}_3$  is isostructural with  $\text{Cr}_2\text{O}_3$ , Fe(III) in the outer layer may easily be substituted by Cr(III) in the lattice and subsequently Cr(III) oxidizes to Cr(VI). The presence of Cr(VI) in the passive film on Fe-Cr alloys [24, 38–41, 44–46] and on AlCr alloys [41, 47] at high positive potentials was demonstrated using the XANES [24, 39–41, 47] and XPS [44–46] techniques. In passive films on SS304, Cr(VI) was found to be formed and enriched in the solid state under the Fe-rich layer [44, 45]. In the case of the Al-Cr alloy [47], the stepping of the potential over a critical value resulted in Cr being incorporated into the Al oxide matrix in such a way that it was stable and could further oxidize to Cr(VI) without dissolving. According to the semiconductor [21], the oxidation of Cr(III) to Cr(VI) is expected to take place in the outer part of the film. The  $\text{CrO}_4^{2-}$  species were not found in the extreme outer part of the film [46] but appeared to populate the  $\text{Cr}(\text{OH})_3$  region below the outermost surface. It is assumed that  $\text{CrO}_4^{2-}$  ions are lost by selective dissolution. Ageing has a beneficial effect on the stability of the passive layer and on the resistance to pitting [48], the latter being directly related to changes in the chemical composition of passive films.

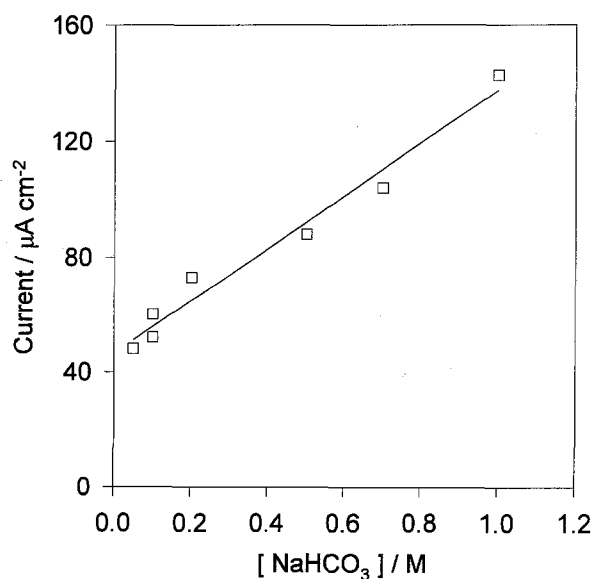


Fig. 5. Effect of  $\text{NaHCO}_3$  solution concentration on anodic current maximum in positive potential region. SS304 electrode rotated at 1000 r.p.m.,  $dE/dt = 0.005 \text{ V s}^{-1}$ , pH 8.

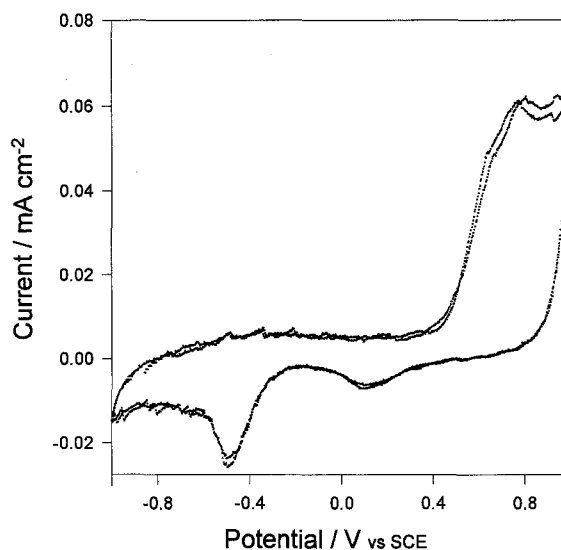


Fig. 6. Cyclic voltammograms for SS304 electrode rotated at 1000 r.p.m.,  $dE/dt = 0.02 \text{ V s}^{-1}$ , in a borate solution at pH 8.

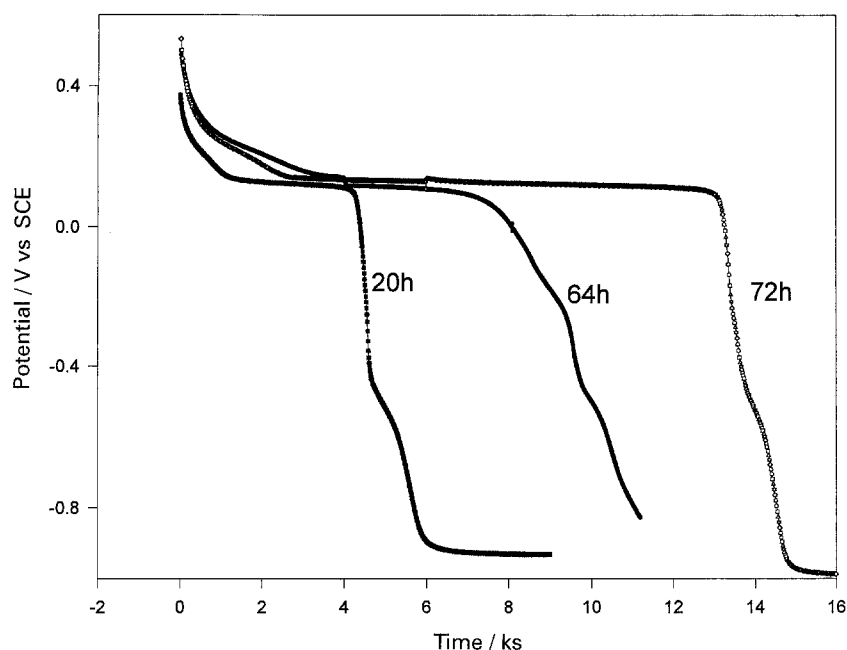


Fig. 7. Effect of oxidation time on passive film formation on the SS304 electrode characterized using the galvanostatic technique. The anodic potential step was applied from  $-0.8$  to  $0.7$  V and after 20, 64 and 72 h oxidation, the measurements were performed at  $8 \mu\text{A cm}^{-2}$ . The electrode rotated at 1000 rpm in 1 M  $\text{NaHCO}_3$  solution at pH 8.

In the present investigation, a series of experiments was performed to study the effect of the oxidation potential, charge and time on passive film formation at potentials above  $+0.4$  V. The anodic film was formed on the rotating disc electrode by applying a potential step from  $-0.8$  V to a high positive potential, and the nature and amount of the oxidation species were deduced from the reduction current waves using potentiodynamic and galvanostatic techniques. Figs 7 and 8 show the effect of the oxidation time on the passive film formation for an applied potential of  $0.7$  V on the SS304 electrode in 1 M  $\text{NaHCO}_3$  solution. In Fig. 7, the surface films were characterized using the galvanostatic reduction technique; the experiments were performed at  $8 \mu\text{A cm}^{-2}$  and the results presented correspond to oxidation times of 20, 64 and 72 h. The high reduction current or the long time needed for performing the galvanostatic measurements had a detrimental effect on their sensi-

tivity; the voltammetric technique was more sensitive. The potentiodynamic traces of Fig. 8 were recorded after 600 s, 20, 72 and 170 h of oxidation and a subsequent negative-going potential scan  $0.05 \text{ V s}^{-1}$ . The amount of anodic products, evaluated from the charge of the cathodic current waves, increased with the oxidation time. Simultaneously with the increase in the cathodic current peak I at about  $0$  V, the current peak II at  $-0.6$  V also increases, indicating that the product reduced at current peak I is at a higher oxidation state. It is supposed that the  $\text{Fe}(\text{VI})$  species appears at positive potential (close to oxygen evolution). The potential of current peak II remained unchanged but that of current peak I shifted in a positive direction, indicating that the anodic product changed with the oxidation time; as the amount of product was accumulated, the corrosion product was easily reduced.

To compare the behaviour of passive films formed

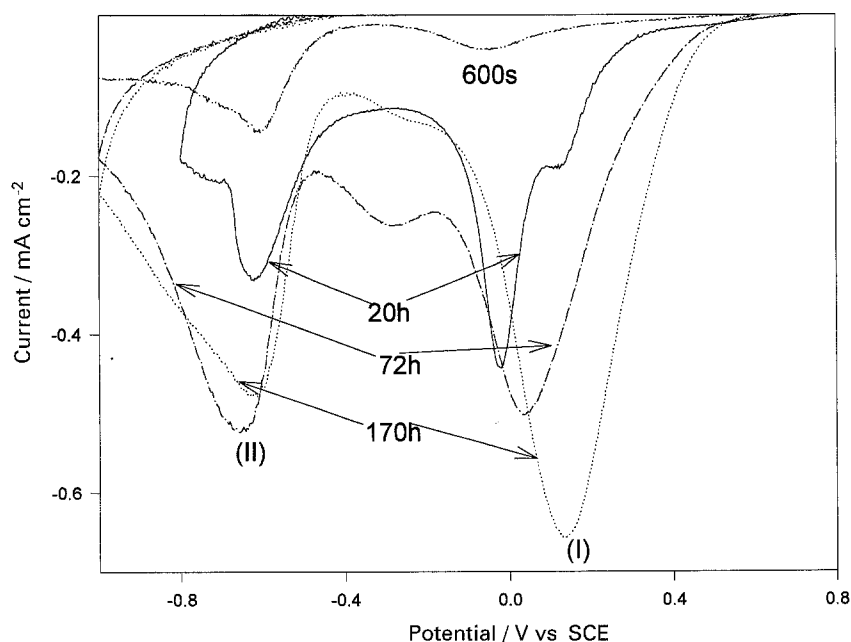


Fig. 8. Effect of oxidation time on passive film formation on the SS304 electrode. The anodic potential step was applied from  $-0.8$  to  $0.7$  V, and the amount of products, after 600 s, 20, 72 and 170 h oxidation time, was evaluated by subsequent cycling of the potential in a negative direction at a scan rate of  $0.05 \text{ V s}^{-1}$ . The electrode was rotated at 1000 r.p.m. in 1 M  $\text{NaHCO}_3$  solution at pH 8.

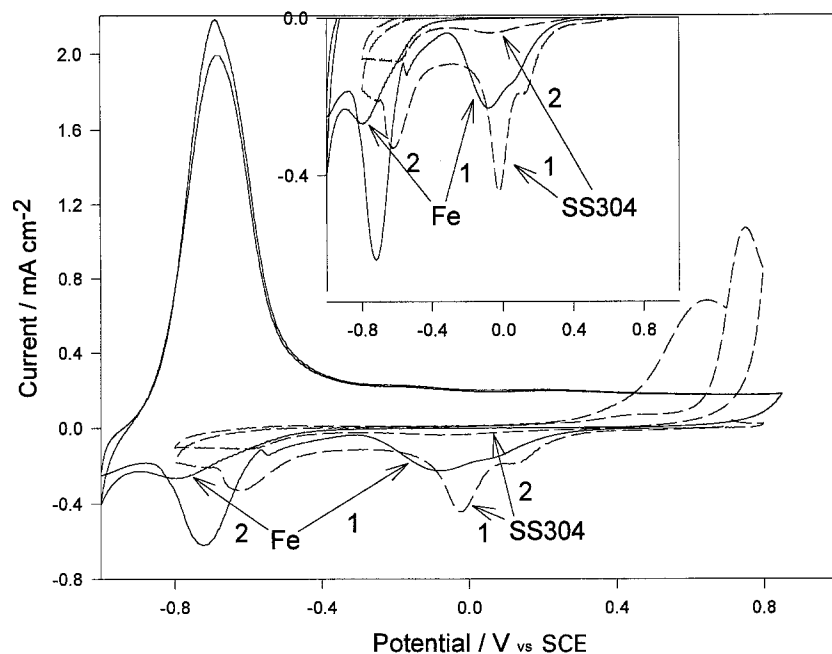


Fig. 9. Effect of 20 h oxidation time on passive film formation on the SS304 electrode in 1 M NaHCO<sub>3</sub> solution and the Fe electrode in 0.5 M NaHCO<sub>3</sub> solution. An anodic potential step from  $-0.8$  to  $0.7$  V was applied, and the amount of products was determined by subsequent cycling of potential, first in a negative then in a positive direction with a scan rate of  $0.05$  V s<sup>-1</sup>. Two cycles are shown. The electrodes were rotated at 1000 r.p.m. in solutions at pH 8. An enlargement of the cathodic side is shown in the insert.

on SS304 and Fe electrodes, measurements were performed after a constant oxidation time and a comparable oxidation charge. It should be noted that special care was taken to avoid contamination by chromium. The voltammograms after 20 h oxidation of SS304 in 1 M NaHCO<sub>3</sub> and Fe in 0.5 M NaHCO<sub>3</sub> solutions are presented in Fig. 9 and for an oxidation charge of  $40$  mC cm<sup>-2</sup> for both electrodes in 1 M NaHCO<sub>3</sub> solution in Fig. 10. When an anodic potential step from  $-0.8$  to  $+0.7$  V was applied to the SS304 and Fe electrodes, the anodic current transient dropped to a stable low value of less than  $1$   $\mu$ A cm<sup>-2</sup>, within few minutes. However, the oxidation current remained much higher for the Cr electrode (i.e.,  $15$   $\mu$ A cm<sup>-2</sup> after 20 h of oxidation). The shape of the cathodic sides of the voltammetric curves was similar for the SS304 and Fe electrodes. The largest increase in the

cathodic charge was observed for the surface product reduced at  $0.1$  V. This cathodic wave corresponds to the reduction of compounds formed at a high positive potential, located in the second passivity region. The film thickens for longer oxidation times, for example, for the SS304 electrode, the reduction charge increased from  $0.3$  mC cm<sup>-2</sup> for 600 s to  $4.5$  mC cm<sup>-2</sup> for 72 h, although for the Fe electrode the charge increases faster than for the SS304 electrode. Under the experimental conditions of Fig. 10, the  $40$  mC cm<sup>-2</sup> oxidation charge required an oxidation time of 72 h for SS304 compared to 20 h for iron, and a comparable reduction charge-related to the current peak at  $0.1$  V was obtained for both electrodes. Reduction current peak II at  $-0.6$  V, which increases as the cathodic current peak I becomes larger, is attributed to the reduction of Fe(II) products. It should be noted that a

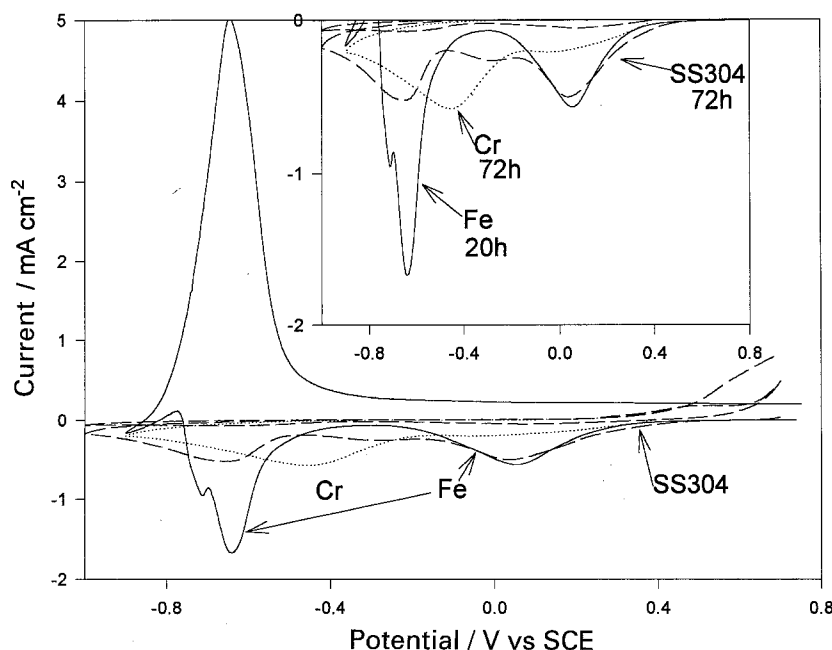


Fig. 10. Effect of an oxidation charge of  $40$  mC cm<sup>-2</sup> on passive film formation on the SS304 and Fe electrodes. The anodic step potential from  $-0.8$  to  $0.7$  V was applied, and the amount of product was determined by subsequent cycling of potential, first in a negative and then in a positive direction, at a scan rate of  $0.05$  V s<sup>-1</sup>. The results for the Cr electrode oxidized to  $900$  mC cm<sup>-2</sup> (72 h) are also shown for comparison. The electrodes were rotated at 1000 r.p.m. in 1 M NaHCO<sub>3</sub> solution at pH 8.

900 mC cm<sup>-2</sup> oxidation charge was measured for the Cr electrode in 1 M NaHCO<sub>3</sub> solution after 72 h oxidation time and the cathodic characteristics were very different, as pointed out above.

The surface of SS304, mild steel 1024 and iron rotating electrodes, anodically polarized at potentials greater than 0.5 V for an oxidation charge greater than 20 mC cm<sup>-2</sup> changed colour to a brilliant gold. The similar appearance of a gold colour was noticed in the bicarbonate as well as in the borate solutions. (Special care was taken to avoid any contamination by chromium). The film adhered well and, after rinsing and drying, the electrode surface film remained unaffected in contact with air. The gold colour was stable in the solution only under the anodic potentials above 0.5 V but it disappeared at open-circuit potential and was easily reduced at about 0.1 V in the first negative-going potential scan.

The overall results indicate that the characteristics of SS304 surface films are a strong function of the applied potential. The electrochemical and chemical reactions occur simultaneously, and the oxidation time and charge are very significant parameters. Since, at high positive potentials, Fe(III) oxides/hydroxides are substantially less soluble than Cr<sub>2</sub>O<sub>3</sub>/Cr(OH)<sub>3</sub>, the iron compounds should be an integral part of the passive film. Fe(III) may further oxidize to Fe(VI) and, by analogy with Cr(VI), a small amount of this species may be incorporated or adsorbed into the passive film. The ferrate ion is relatively stable in basic solution, but in neutral and acidic solution it decomposes. It is an extremely potent oxidizing agent, even stronger than permanganate, and it can oxidize Cr(III) to chromate. Potassium ferrate has been shown to be isomorphous with potassium chromate. According to kinetic data [49] the free ferrate in solution is highly stabilized in concentrated NaOH solutions and decomposes more slowly (by a factor of 10<sup>5</sup>) than the surface Fe(VI) complex. A transpassive anodic current peak, preceding the oxygen evolution, has been detected on mild steel in aqueous bicarbonate/carbonate solutions at pH 10–13 [50, 51]. An increase in the peak current with increasing temperature was also indicative that a chemical reaction was involved. The formation of Fe(VI) species was proposed and it was found that HCO<sub>3</sub><sup>-</sup> ions stabilize the superficial ferrate. The free ferrate would decompose faster in bicarbonate/carbonate than in NaOH solutions due to the pH requirements.

In the present investigation, part of the passive films is most likely formed by the dissolution and precipitation of ferric oxides/hydroxides or oxyhydroxides, although for extended oxidation time active dissolution is inhibited and oxidation via a direct growing passive film becomes important. The surface film is saturated with iron and oxygen. Under such conditions, and since the composition of passive films is potential dependent and the surface species may be stable only under high positive potential or when dehydrated, the film of Fe(III) compounds with incorporated or adsorbed Fe(VI) species must be responsible

for passivation of the SS304 electrode surface at potentials above 0.5 V.

#### 4. Conclusion

Two types of passive films of different chemical composition on the surface of the SS304 electrode are proposed. In the low potential range, the electrode behaves like a Cr-rich metallic phase. The dissolution of Fe<sup>2+</sup> ions into the solution is hindered by the formation of a chromium oxide/oxyhydroxide layer. The low anodic current in the passive regions is independent of the bicarbonate solution concentration.

The passive film is partially dissolved at 0.4 V by the oxidation-dissolution reaction of Cr(III) to CrO<sub>4</sub><sup>2-</sup>, which depends on the carbonate solution concentration. At potentials above 0.4 V, the dissolution of chromium and subsequent surface enrichment of iron suggest that Fe(III) oxide/oxyhydroxide films, with Fe(VI) species incorporated or adsorbed in the films, are responsible for SS304 passivation. Since the electrochemical and chemical reactions occur simultaneously, the increase in the overall thickness of the film is time dependent.

Colouration of stainless steel, mild steel and iron was observed in carbonate/bicarbonate and borate solutions. The identity of the coloured passive film is a strong function of applied high positive potential, anodic charge and time. The components of the passive film are referred as a mixed-valence and mixed-iron species and their stoichiometry is not stable. The uniform gold colour of the surface film remains unchanged in air and in the solution under potentials above 0.5 V but disappears at open-circuit potential and is easy to remove in the negative-going potential scan.

#### Acknowledgements

This research was supported by Hydro-Québec (IREQ) and the Natural Sciences and Engineering Research Council of Canada.

#### References

- [1] K. E. Heusler, in 'Encyclopedia of the Electrochemistry of Elements', (edited by A. J. Bard) Marcel Dekker, New York (1986).
- [2] P. Southworth, A. Hamnett, A. M. Riley and J. M. Sykes, *Corros. Sci.* **28** (1988) 1139.
- [3] T. E. Graedel and R. P. Frankenthal, *J. Electrochem. Soc.* **137** (1990) 2385.
- [4] J. Gui and T. M. Devine, *Corros. Sci.* **36** (1994) 441; *ibid.* **32** (1991) 1105. *J. Electrochem. Soc.* **138** (1991) 1376.
- [5] M. G. S. Ferreira and J. L. Dawson, *J. Electrochem. Soc.* **132** (1985) 760.
- [6] S. Virtanen, E. M. Moser and H. Böhni, *Corros. Sci.* **36** (1994) 373.
- [7] S. Virtanen, J. Böhni, *Materials Science Forum*, accepted.
- [8] J. H. Gerretsen, J. H. de Wit and J. C. Rivière, *Corros. Sci.* **31** (1990) 545.
- [9] S. Govindarajan and H. Cragolino, *J. Electrochem. Soc.* **134** (1987) 2986.
- [10] C. Humschmid and D. Landolt, in 'Oxide Films on Metals



- and Alloys' (edited by B. R. MacDougall, R. S. Alwitt and T. A. Ramanarayanan) The Electrochemical Society, Pennington, NJ (1992), p. 187.
- [11] K. Ogura, M. Tsujigo, K. Sakurai and J. Yano, *J. Electrochem. Soc.* **140** (1993) 1311.
- [12] C. Y. Chao, L. F. Lin and D. D. Macdonald, *ibid.* **129** (1982) 1874.
- [13] S. Silverman, G. Cragnolino and D. D. Macdonald, *ibid.* **129** (1982) 2419.
- [14] A. Di Paola, *Electrochim. Acta* **34** (1989) 203; *Corros. Sci.* **31** (1990) 739.
- [15] A. M. P. Simões, M. G. S. Ferreira, G. Lorang and M. da Cunha Belo, *Electrochim. Acta* **36** (1991) 315.
- [16] M. G. S. Ferreira, T. Moura e Silva, A. Catarino, M. Pankuch and C. A. Melendres, *J. Electrochem. Soc.*, **139** (1992) 3146.
- [17] C. A. Melendres, M. Pankuch and M. G. S. Ferreira, in 'Oxide Films on Metals and Alloys', *op. cit.* [10], p. 1.
- [18] R. Babić, M. Metikoš-Huković, *J. Electroanal. Chem.* **358** (1993) 143.
- [19] A. M. P. Simões, M. G. S. Ferreira, B. Rondot and M. da Cunha Belo, *J. Electrochem. Soc.* **137** (1990) 82.
- [20] U. Stimming, in 'Passivity of Metals and Semiconductors' (edited by M. Froment) Elsevier Science, Amsterdam (1983), p. 509. *Electrochim. Acta* **31** (1986) 415.
- [21] P. Schmuki and H. Böhm, *J. Electrochem. Soc.* **139** (1992) 1908; *ibid.* **141** (1994) 362; *idem* in 'Oxide Films on Metals and Alloys', *op. cit.* [10], p. 326.
- [22] H. H. Strehblow, *Surf. Interf. Anal.* **12** (1989) 363.
- [23] I. Olefjord and L. Wegelius, *Corros. Sci.* **31** (1990) 89.
- [24] A. J. Davenport, M. Sansone, J. A. Bardwell, A. J. Aldykiewicz, Jr., M. Taube and C. N. Vitus, *J. Electrochem. Soc.* **141** (1994) L6.
- [25] E. Deltombe and M. Pourbaix, 'Compartement Electrochimique du Fer en Solution Carbonique, Diagrammes d'Equilibre Tension-pH du Systeme Fe-CO<sub>2</sub>-H<sub>2</sub>O a 25 °C', CEBELCOR, Rapport Technique No 8 (1954).
- [26] M. Pourbaix, 'Atlas of Electrochemical Equilibria in Aqueous Solutions', NACE, Texas (1974).
- [27] A. J. Bard, R. Parsons, J. Jordan (eds), 'Standard Potentials in Aqueous Solutions', M. Dekker, New York (1985) p. 453.
- [28] G. H. Kelsall, C. I. House and F. P. Gudyanga, *J. Electroanal. Chem.* **244** (1988) 179.
- [29] N. Hara and K. Sugimoto, *J. Electrochem. Soc.* **126** (1979) 1328.
- [30] S. Haupt and H. H. Strehblow, *J. Electroanal. Chem.* **216** (1987) 229; *ibid.* **228** (1987) 365.
- [31] M. Metikoš-Huković, M. Ceraj-Cerić, *J. Electrochem. Soc.* **134** (1987) 2193.
- [32] C. A. Melendres, M. Pankuch, Y. S. Li and L. R. Knight, *Electrochim. Acta* **37** (1992) 2747.
- [33] M. Seo, R. Saito and N. Sato, *J. Electrochem., Soc.* **127** (1980) 1909.
- [34] T. P. Moffat and R. M. Latanision, *ibid.* **139** (1992) 1869.
- [35] L. Bjornkvist and I. Olefjord, *Corros. Sci.* **32** (1991) 231.
- [36] B. Stypula and J. Banaś, *Electrochim. Acta* **38** (1993) 2309.
- [37] G. H. Sillén and A. E. Martell, 'Stability Constants of Metal-Ion Complexes', Special Publication 17, The Chemical Society, London (1964); 'CRC Handbook of Chemistry and Physics', 74th edn (edited by D. R. Lide), CRC Press, London (1993).
- [38] J. A. Bardwell, G. I. Sproule, B. MacDougall, M. J. Graham, A. J. Davenport and H. S. Isaacs, *J. Electrochem. Soc.* **139** (1992) 371.
- [39] J. A. Bardwell, G. I. Sproule, D. F. Mitchell, B. MacDougall and M. J. Graham, *J. Chem. Soc. Faraday Trans.* **87** (1991) 1011.
- [40] G. G. Long, J. Kruger and D. Tanaka, *J. Electrochem. Soc.* **134** (1987) 264.
- [41] J. Davenport, H. S. Isaacs, G. S. Frankel, A. G. Schrott, C. V. Jahnes and M. A. Russak, *J. Electrochem. Soc.* **138** (1991) 337.
- [42] W. P. Yang, D. Costa and P. Marcus, in 'Oxide Films on Metals and Alloys', *op. cit.* [10], p. 516.
- [43] D. Landolt, in 'Passivity of Metals' (edited by R. P. Frankenthal and J. Kruger), The Electrochem. Society, Princeton, NJ (1978) p. 484.
- [44] C. Calinski and H. H. Strehblow, *J. Electrochem. Soc.* **136** (1989) 1328.
- [45] A. R. Brooks, C. R. Clayton, K. Doss and Y. C. Lu, *ibid.* **133** (1986) 2459.
- [46] C. R. Clayton and Y. C. Lu, *ibid.* **133** (1986) 2465.
- [47] G. S. Frankel, A. G. Schrott, A. J. Davenport, H. S. Isaacs, C. V. Jahnes and M. A. Russak, *ibid.* **141** (1994) 83.
- [48] W. P. Yang, D. Costa and P. Marcus, *ibid.* **141** (1994) 111.
- [49] F. Beck, R. Kaus and M. Oberst, *Electrochim. Acta* **30** (1985) 173.
- [50] C. M. Rangel, I. T. Fonseca and R. A. Leitão, *ibid.* **31** (1986) 1659.
- [51] C. M. Rangel and R. A. Leitão, *ibid.* **34** (1989) 255.